A PLANAR-LUMPED MODEL FOR COUPLED MICROSTRIP LINE DISCONTINUITIES

Albert Sabban and K.C Gupta

Department of Electrical and Computer Engineering
University of Colorado at Boulder

Abstract

This paper presents a convenient model for analyzing coupled microstrip line discontinuities. Similar to the planar magnetic wall model for single microstrip lines, a planar-lumped model is developed for coupled microstrip lines. Fields underneath the two strips and those fringing at the outer edges are modeled by equivalent planar waveguides. Electric and magnetic field coupling in the gap region is modeled by a lumped network. Model parameters are evaluated such that [C] and [L] matrices of the model are identical with those of coupled lines. This modeling approach is applied to a coupled microstrip section with chamfered right-angled bends to single microstrip lines, and results are in good agreement with experimental values.

Introduction

Although characteristics of uniform coupled lines have been studied extensively[1], characterization of discontinuities and junctions in coupled lines is not readily available. Specifically, there is a need for characterization of junctions between coupled line sections and outgoing single microstrip lines.

The purpose of this paper is to present a model suitable for characterization of several of the coupled-line junction configurations. The role of this model is similar to that of the planar waveguide model for single microstrip lines, the model that has been used extensively for characterization of several microstrip discontinuities like bends, chamfered bends, tee-junctions and cross-junctions etc.[2, 3]. The proposed model is a combination of two-dimensional planar and lumped-element networks. Fields underneath the two strips and those fringing at the outer-edges are modeled by planar waveguides. The electric field and magnetic field coupling across the gap are represented by an equivalent capacitive and inductive lumped network.

Planar-Lumped Model

A coupled microstrip line section and its planar-lumped model is shown schematically in Figure 1. Fields underneath the two strips and fringing fields at the outer edges e_1 and e_2 are represented by two planar waveguides (with magnetic walls) characterized by Z-matrices Z_A and Z_B respectively. Selection of various parameters ensures that the capacitances and inductance matrices for the coupled line configuration and its model are identical.

Planar Waveguides' Parameters: For a single microstripline, effective width in the planar waveguide model [5] is given by

$$W_{em}(f) = \eta_0 h / \left\{ Z_0(f) \sqrt{\varepsilon_{re}(f)} \right\} \quad (1)$$

where η_o is the intrinsic wave impedance (120π ohms) of free space and h is the height of the substrate. $Z_o(f)$ and $\varepsilon_{re}(f)$ are the frequency dependent characteristic impedance and effective dielectric constant values obtained from microstrip line analysis. The planar waveguide of height h and width $W_{em}(f)$ is bounded by two magnetic walls on the sides and there are no fields outside this region. The medium inside the planar waveguide has a dielectric constant equal to $\varepsilon_{re}(f)$. Model parameters are selected such that L and C per unit length of the microstrip line and the model are equivalent. This modeling approach has been successful in analysis of microstrip discontinuities and junctions[2, 3].

For the coupled microstrip line model, the planar waveguides account for fringing fields only at the outer edges. So their effective widths $W_e(f)$ are chosen as

$$W_e(f) = \frac{W_{em}(f) + W}{2} \quad (2)$$

where W is the physical width for the two coupled lines. The dielectric constant of planar waveguide segments is taken to be equal to ε_{re} for a microstrip line of width W. The two planar waveguide segments are connected together through a multiport lumped network as shown in Figure 1. Usually, 25 ports per quarter wavelength are needed to ensure matching of the fields under the strips to that in the gap region. Z-matrices for two planar segments are derived from two-dimensional Green's function for rectangular geometry and account for all the higher (z-invariant) two-dimensional modes present in these regions.

C-Network for Modeling E-Field Coupling: The lumped network representing the electric field coupling between the two strips is derived from the capacitance matrix of the coupled microstrip line. The Bryant and Wiess[4] algorithm was used for computation of the C-matrix. Even and odd mode capacitances (C_e and C_o respectively) are related to the [C] matrix as follows:

$$[C] = \begin{bmatrix} C_{11} & -C_{11} \\ -C_{21} & C_{22} \end{bmatrix} = \begin{bmatrix} C_e & (C_0 - C_e)/2 \\ (C_0 - C_e)/2 & C_e \end{bmatrix} \quad (3)$$

A π-network representation of the [C] matrix is shown in Figure 2(a). In the model proposed (Figure 1), C_{11} is accounted for partially by the planar segment (with $[Z] = Z_A$). The remaining part of C_{11} is modeled by the element C_f of the lumped network, shown in Figure 2(b).

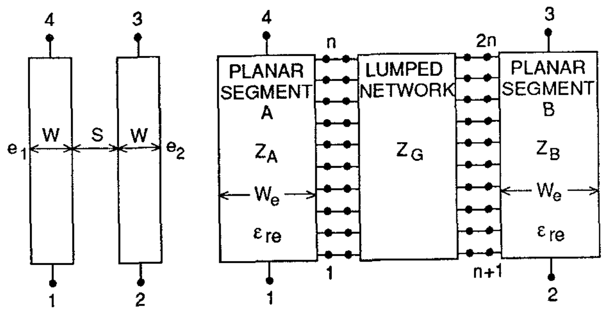

Figure 1: A coupled line section and its planar-lumped model.

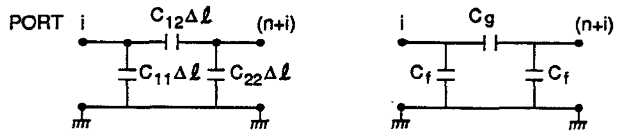

(a) (b)

Figure 2(a): π-matrix representation of [C] for coupled lines.

Figure 2(b): A section of the capacitive port of the lumped network.

We get

$$C_f = \left(C_{11} - \frac{\varepsilon_o \varepsilon_{re} W_e}{h}\right)\Delta\ell = \left(C_e - \frac{\varepsilon_o \varepsilon_{re} W_e}{h}\right)\Delta\ell \qquad (4)$$

$\Delta\ell$ is the length of the line represented by the port i. The matrix [C] represents capacitances per unit length of the line. The network section shown in Figure 2(b) may be represented by the following matrix:

$$[Y_c] = j\omega\begin{bmatrix} C_f + C_g & -C_g \\ -C_g & C_f + C_g \end{bmatrix} = j\omega[C_G] \qquad (5)$$

When the lumped network of Figure 1 has n ports on each side, the complete C-matrix $[C_G]$ may be written as shown in Table 1. Non-diagonal terms in each of the four sub-matrices are all zeros.

<u>L-Network for Modeling H-Field Coupling</u>: The magnetic field coupling between the two strips is modeled by mutual inductance elements in the lumped network. If we consider two adjacent ports of planar segment A (say 1 and 2) connected to the two corresponding ports (n+1 and n+2) of the segment B, the inductive network for this portion may be drawn as shown in Figure 3(a).

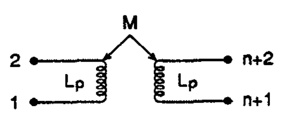

Figure 3(a): A section of the inductive network in the lumped network.

Table 1: C-matrix for the lumped network modeling the gap.

$$[C_G] = \begin{array}{c} \\ 1 \\ \vdots \\ n \\ n+1 \\ \vdots \\ 2n \end{array} \left[\begin{array}{cccc|cccc} 1 & \cdots & & n & n+1 & \cdots & & 2n \\ C_f+C_g & & & & -C_g & & & \\ & \ddots & & & & \ddots & & \\ & & & C_f+C_g & & & & -C_g \\ \hline -C_g & & & & C_f+C_g & & & \\ & \ddots & & & & \ddots & & \\ & & & -C_g & & & & C_f+C_g \end{array}\right]$$

Values of L_p and M are calculated by comparing the [L] matrix of the coupled line with that for the modeling network. The inductance matrix for the coupled line pair is obtained from the capacitance matrix $[C_o]$ for the case when the dielectric is replaced by air. We have the following relation[5] between [L] and $[C_o]$:

$$[L] = \mu_o \varepsilon_o [C_o]^{-1} = \begin{bmatrix} L_{11} L_{12} \\ L_{21} L_{22} \end{bmatrix} \qquad (6)$$

where μ_o and ε_o are permeability and permitivity of the free space. The network representation of the inductance matrix in equation (6) is shown in Figure 3(b). Here $\Delta\ell$ is the length of the section represented by the partial network shown and [L] is the matrix of inductances per unit length of the coupled line pair. A part of the $\Delta\ell L_{11}$ is contributed by the inductance of the parallel plate waveguide and the remaining by L_p included in the lumped network as shown in Figure 3(a). If the inductance of the parallel plate waveguide region per unit length ($= \mu_o h/W_e$) is denoted by $L_{p\ell}$, the total inductance network may be drawn as shown in Figure 3(c). Equating the admittance matrices of the two networks shown in Figure 3(b) and 3(c), L_p and M may be expressed in terms of $L_{p\ell}$ and [L] as follows:

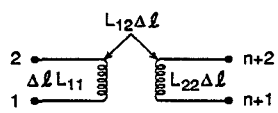

Figure 3(b)

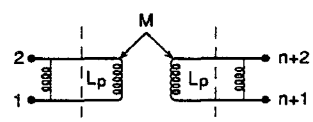

Figure 3(c)

Figure 3(b):Network representation network for inductive matrix

Figure 3(c): Total inductance network

$$L_p = \frac{L_{11} - (L_{11}^2 - L_{12}^2)/L_{p\ell}}{1 - 2L_{11}/L_{p\ell} + (L_{11}^2 - L_{12}^2)/L_{p\ell}^2}\Delta\ell \qquad (7)$$

and

$$M = \frac{L_{12}\Delta\ell}{1 - 2L_{11}/L_{p\ell} + \left(L_{11}^2 - L_{12}^2\right)/L_{p\ell}^2} \qquad (8)$$

In (7) and (8), it is assumed that $L_{11} = L_{22}$ and that $L_{12} = L_{21}$ (symmetric lines). Formulation could, of course, be extended to asymmetric lines also. For the complete lumped network portion of the model, the inductive part is represented by a (2n x 2n) admittance matrix which is obtained by using Kirchoff's laws and may be written as follows:

$$[Y_L] = \frac{-j}{\omega\left(L_p^2 - M^2\right)}[L_G] \qquad (9)$$

where $[L_G]$ is (2n x 2n) inductance matrix shown in Table 2. It may be noted that all the four (n x n) sub-matrices are tridiagonal, all other elements being zero.

Table 2: L-matrix for the lumped network modeling the gap

$$[L_G] = \begin{array}{c} \\ 1 \\ 2 \\ 3 \\ \vdots \\ \\ n-1 \\ n \\ n+1 \\ n+2 \\ n+3 \\ \vdots \\ \\ 2n-1 \\ 2n \end{array} \left[\begin{array}{cccccc|cccccc}
1 & 2 & 3 \cdots & & n-1 & n & n+1 & n+2 & n+3 \cdots & & 2n-1 & 2n \\
L_p & -L_p & 0 & & & & -M & M & 0 & & & \\
-L_p & 2L_p & -L_p & & & & M & -2M & M & & & \\
0 & -L_p & 2L_p & \ddots & & & 0 & M & -2M & \ddots & & \\
& & \ddots & \ddots & \ddots & & & & \ddots & \ddots & \ddots & \\
& & & 2L_p & -L_p & 0 & & & & -2M & M & 0 \\
& & & -L_p & 2L_p & -L_p & & & & M & -2M & M \\
& & & 0 & -L_p & L_p & & & & 0 & M & -M \\
\hline
-M & M & 0 & & & & L_p & -L_p & 0 & & & \\
M & -2M & M & & & & -L_p & 2L_p & -L_p & & & \\
0 & M & -2M & \ddots & & & 0 & -L_p & 2L_p & \ddots & & \\
& & \ddots & \ddots & \ddots & & & & \ddots & \ddots & \ddots & \\
& & & -2M & M & 0 & & & & 2L_p & -L_p & 0 \\
& & & M & -2M & M & & & & -L_p & 2L_p & -L_p \\
& & & 0 & M & -M & & & & 0 & -L_p & L_p
\end{array}\right]$$

The total lumped network required for modeling the gap is obtained by superposition of capacitance and inductive components. The total admittance matrix of this network is obtained by adding $[Y_C]$ and $[Y_L]$ given by equations (5) and (9) respectively. We have the admittance matrix of the gap network Y_G given by:

$$[Y_G] = [Y_c] + [Y_L] = j\omega[C_G] - \frac{j}{\omega\left(L_p^2 - M^2\right)}[L_G] \qquad (10a)$$

$$[Z_G] = [Y_G]^{-1} \qquad (10b)$$

Model Verification

The planar-lumped model for coupled microstrip lines proposed in this paper has been verified by considering a quarter-wave section of coupled line, finding its 4-port parameters based on the proposed model, and comparing these with the four-port parameters obtained by conventional coupled line analysis[6]. The starting point for both of these computations is the values of the even and odd-mode impedance and effective dielectric constants obtained from the Bryant and Wiess algorithm[4].

In conventional coupled-line computations, non-equality of even and odd-mode phase velocities has been taken into account. The configuration considered is a pair of microstrip lines (each 50Ω characteristic impedance in isolation) on 0.01 inch thick substrate with $\varepsilon_r = 2.2$ and their lengths equal to λ/4 at 10GHz. Coupling values were calculated for spacing varying from 0.1 to 20 times the substrate thickness and the coupling parameters S_{21} calculated for various cases.

For computations based on the proposed model, some further details need to be mentioned. For Z-matrices for rectangular segments, single summation formulation[7] has been used. The number of terms needed for convergence was decided by iterative computations to be around 100. Optimum width of the ports interconnecting these rectangular segments to the gap network is found to be λ/100. Segmentation method[3] was used to combine the Z-matrices of the two planar segments and that of the gap into a single 4x4 Z-matrix (with respect to the four external ports). The Z-matrix for the coupled line section is converted into a 4x4 S-matrix.

The four-port S-matrices obtained by these two approaches agree very well. Comparison for the case of coupling coefficient S_{12} is shown in Figure 4. The two curves coincide and cannot be distinguished in the figure.

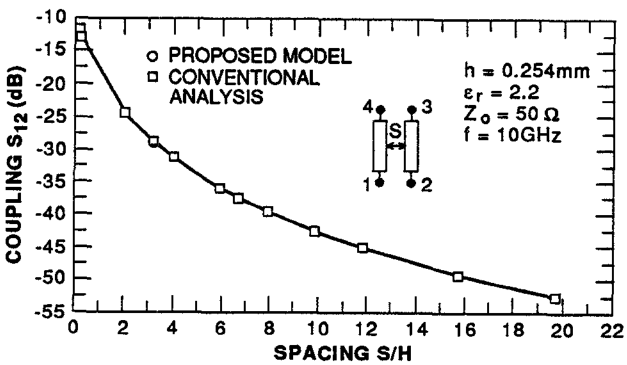

Figure 4: Comparison of coupling computed by planar lumped model with transmission line equations.

Comparison with Experiment for Chamfered Bends

The coupled line model proposed above has been applied for characterization of the junction between coupled line section and single microstrips located at right angles to ends of the coupled line section as shown in Figure 6 (inset). The planar/lumped model of this configuration is shown in Figure 5. In addition to the three segments (two rectangular plus a lumped network) representing the coupled line section, we have three additional planar segments at each of the two upper ports (1 and 2).

The analysis procedure for this configuration may be summarized as follows: (i) Thirty ports on each side connect lumped network to planar segments. The number of interconnections between segments 1 and 2, 2 and 3, and 3 and 4 (and similarly on the right-hand side) is about seven each; (ii) Z-matrices for various segments are evaluated from corresponding Green's functions. For isosceles triangles a single summation formulation[8] is used. Y-matrix for lumped network is obtained as discussed earlier; (iii) These Z-matrices are combined using the segmentation formula to obtain a 4x4 Z-matrix; (iv) 4x4 Z-matrix is reduced to 2x2 matrix with ports 3 and 4 terminated in 50Ω resistances; (v) 2x2 Z-matrix is converted to S-matrix.

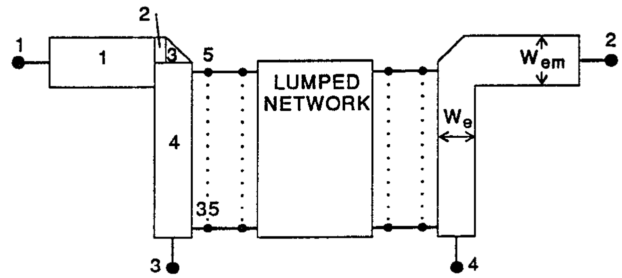

Figure 5: Planar model for chamfered bend coupled line.

The results obtained by the above procedure are compared with the experimental results for the structure fabricated on 4 mil thick GaAs substrate (ε_r = 12.9). Comparison for the transmission coefficient S_{21} is shown in Figure 6. The curve marked 1 shows computed results, curve 3 shows experimental results, and curve 2 shows the results without taking junction reactance into account. The data for curve 2 is obtained from transmission line analysis of coupled lines.

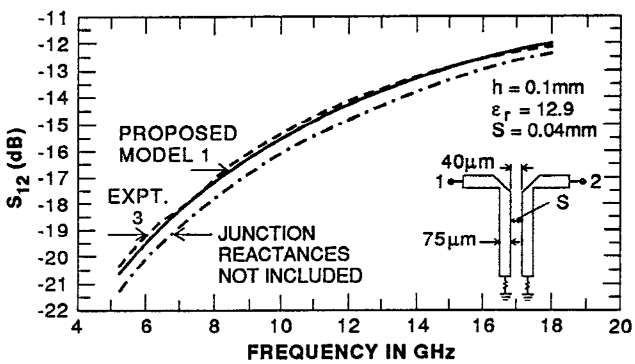

Figure 6: Comparison of S_{12} values for chamfered bend coupled line as obtained from planar model, from measured results, and from transmission line equations with no discontinuity reactances included.

Good agreement between computed and experimental results verifies the modeling procedure developed and its applications to analysis of coupled line discontinuities.

Concluding Remarks

A novel modeling approach for characterization of coupled microstrip junction effects has been reported in this paper. This approach is an extension of the planar waveguide model used extensively for single microstrip line discontinuity reactance characterization. Good agreement with experimental results for chamfered bends (between coupled lines and single microstrip lines) is very encouraging.

The proposed model is applicable to a number of different coupled line structures such as a coupled line section with an abrupt 90° bend connections to single microstrip lines, a coupler with chamfered bends, and a coupler with outgoing lines bent at an angle of only 45°. The proposed model is also applicable to the analysis of step discontinuities between coupled line sections such as encountered in multisectional directional couplers.

Acknowledgements: The authors are grateful to Mr. Steve Yuan for making available the experimental results reported in Figure 6 from the work carried out at Hughes Aircraft Company, Microwave Products Division, Torrance, California.

REFERENCES

[1] R.H. Jansen, "High speed Computation of single and coupled Microstrip Parameters including Dispersion, High order modes, Loss and Finite strip thickness", IEEE Trans. Microwave Theory Tech., vol. MTT-26, February, 1978, pp. 25-82.

[2] G. Kompa and R. Mehran, "Planar waveguide model for computing microstrip components", Electronics Letters, vol. 11, no. 9, 1975, pp. 459-460.

[3] R. Chadha and K.C. Gupta, "Compensation of discontinuities in planar transmission lines", IEEE Trans. Microwave Theory Tech., vol. MTT-30, Dec. 1982, pp. 2151-2156.

[4] J.A. Wiess, "Microwave propagation on coupled pairs of microstrip transmission lines", in Advances in Microwaves, vol. 8 (eds. L. Young and H. Sobol), Academic Press, 1974, pp. 295-320.

[5] L.N. Dworsky, "Modern Transmission Line Theory and Applications", Robert E. Krieger Publishing Company, Malabar, Florida, 1988, pp. 109-136.

[6] K.C. Gupta, "Microwaves", John Wiley Halstad Press, 1980, Chapter 7.

[7] A. Benalla and K.C. Gupta, "Faster computation of Z matrices for rectangular segments in planar microwave circuits", IEEE Trans. Microwave Theory and Tech., vol. MTT-34, June 1986, pp. 733-736.

[8] H.J. Maramis and K.C. Gupta, "Planar Model Characterization of Compensated Microstrip Bends", MIMICAD Report #1, University of Colorado at Boulder,1989.